These results were denoted in Figs. 1 and 2 by MR and indicated that not only were more iterations needed, but the CPU time per iteration also took about three times that required for the AF or ZEBRA scheme. Consequently, it was not competitive with the AF scheme. However, by using a more accurate LU factorization (i.e., by introducing more nonzero diagonals into the L and U matrices), a faster convergence rate was achieved. Since the number of iterations for both outer and inner iterations is reduced substantially, the performance of the new MR method (denoted by MR2 in Figs. 1 and 2) is more efficient than the old MR method. A detailed implementation of the improved MR method (including the construction for the preconditioning operator C), and comparisons with the AF scheme for lifting and nonlifting calculations, have been reported by Wong.[7]

Acknowledgments

This work was supported by the National Aeronautics and Space Administration under Contracts NAS-15810 and NAS-16394 while the first author was in residence at the Institute for Computer Applications in Sciences and Engineering (ICASE), NASA Langley Research Center, Hampton, Virginia. The authors wish to thank Terry Holst of NASA Ames, Jerry South of NASA Langley, and Mike Doria of Valparaiso University, for providing them with their codes to test the MR and ZEBRA algorithms. The authors would also like to thank the referees for their comments and suggestions.

References

[1]South, J. C., Keller, J. D., and Hafez, M. M., "Vector Processor Algorithm for Transonic Flow Calculations," *AIAA Journal*, Vol. 18, July 1980, pp. 786-792.

[2]Holst, T. L. and Ballhaus, W. F., "Fast Conservative Schemes for the Full Potential Equation Applied to Transonic Flow," *AIAA Journal*, Vol. 17, Feb. 1979, pp. 145-152.

[3]Khosla, P. K. and Rubin, S. G., "A Conjugate Gradient Iterative Method," *Lecture Notes in Physics*, Vol. 141, Springer-Verlag, New York, 1981, pp. 248-253.

[4]Wong, Y. S. and Hafez, M. M., "Conjugate Gradient Methods Applied to Transonic Finite Difference and Finite Element Calculations," *AIAA Journal*, Vol. 20, Nov. 1982, pp. 1526-1533.

[5]Dougherty, F. C., Holst, T. L., Gundy, K. L., and Thomas, S. D., "TAIR—A Transonic Airfoil Analysis Computer Code," NASA TM 81296, 1981.

[6]Hafez, M. M. and Lovell, D., "Improved Relaxation Schemes for Transonic Potential Calculations," AIAA Paper 83-0372, 1983.

[7]Wong, Y. S., "Newton-Like Minimal Residual Methods Applied to Transonic Flow Calculations,"*AIAA Journal*, Vol. 23, April 1985, pp. 515-521.

Refinement of an "Alternate" Method for Measuring Heating Rates in Hypersonic Wind Tunnels

Charles G. Miller*
NASA Langley Research Center, Hampton, Virginia

Nomenclature

c = specific heat, J/kg-K
C_h = heat-transfer coefficient, $\dot{q}_{t,2}/(T_{t,2}-T_s)$, W/m^2-K
k = thermal conductivity, W/m-K
M = Mach number
p = pressure, N/m^2
$\dot{q}$ = heat-transfer rate, W/m^2
r_n = nose radius, m
R = unit Reynolds number, $\rho U/\mu$, m^{-1}
t = time, s
T = temperature, K
U = velocity, m/s
β = thermal product, $(\rho ck)^{1/2}$, W-s$^{1/2}$/m^2-K
μ = coefficient of viscosity, N-s/m^2
ρ = density, kg/m^3

Subscripts

s = surface or substrate
$t,1$ = reservoir stagnation conditions
$t,2$ = stagnation conditions behind normal shock
2 = static conditions immediately behind normal shock
0 = ambient or initial ($t \leq 0$)
∞ = freestream

Received Jan. 25, 1984; revision received June 12, 1984. This paper is declared a work of the U.S. Government and therefore is in the public domain.

*Aerospace Engineer, Aerothermodynamics Branch, Space Systems Division. Member AIAA.

Introduction

CONVECTIVE heating for proposed Earth or planetary entry vehicles is generally inferred from model tests in hypersonic facilities and flowfield computer codes that often are verified with these or similar heat-transfer measurements. Such measurements are relatively straightforward for models of a simple shape, but difficulties arise for complex models characterized by surfaces with small radii of curvature (e.g., wing leading edge). Accurate measurement of surface heating using conventional transient calorimeter techniques becomes quite challenging for complex models and often is impossible. For this and other reasons, an alternative method for measuring detailed heating distributions on models in conventional-type hypersonic wind tunnels was examined at the Langley Research Center several years ago.[1] Borrowing from technology developed for hypervelocity impulse facilities having extremely short run times (< 10 ms), thin-film resistance gages were successfully tested in hypersonic wind tunnels at the most hostile environment generated in each tunnel. One significant difference between these gages and previous thin-film gages used in impulse facilities was the substrate material. A glass ceramic referred to as MACOR (trademark of Corning Glass Works) was used in lieu of quartz or Pyrex.[2] Because the thermal properties of MACOR are similar to quartz and Pyrex, gage performance is similar; however, unlike quartz and Pyrex which must be ground, MACOR may be machined with conventional metal cutting tools and techniques. Thus, complex surfaces may be machined from MACOR, polished, and miniature thin-film elements sputtered or painted on the surface at a cost substantially less than quartz or Pyrex.

The advantages, disadvantages, limitations, and uncertainties of using thin-film gages in conventional hypersonic wind tunnels having longer run times than impulse facilities by several orders of magnitude are discussed in Refs. 1 and 3. The purpose of this Note is to present recent results that resolve the principal uncertainty associated with the use of thin-film gages on MACOR substrates—the uncertainty in the thermal properties of MACOR and the variation of these properties with temperature. These results are based on stagnation-point heat-transfer rates measured on small hemispheres in hypersonic wind tunnels. Along with providing information on MACOR properties, they also illustrate the relatively large influence of shock strength (normal shock density ratio) on stagnation point heating at low Reynolds numbers.

Apparatus and Tests

The present study was performed in the Langley 31 in. Mach 10 Tunnel[4] (formerly known as the Continuous Flow Hypersonic Tunnel), and the Langley Hypersonic CF_4 Tunnel,[4] a Mach 6 facility that uses Freon 14 to generate a normal

shock density ratio of 12. Five small ($r_n = 4.1$ mm) hemispheres, two of MACOR, two of quartz, and one of Pyrex 7740, were mounted in a survey rake, rapidly injected into the flow (approximately 0.3 s required to traverse the nozzle boundary layer and reach the vicinity of the nozzle centerline), and subjected to the same flow condition at the same time. Palladium thin-film elements in the form of a serpentine pattern 1×1.3 mm were sputtered over the stagnation region of each hemisphere. The same calibration procedure, constant-current circuitry, analog-to-digital data acquisition system, sample rate (each channel sampled 50 times/s), excitation current (1 mA), and data-reduction procedure were used for the five thin-film gages in both tunnels. Thus, the substrate material was the only intended variable for a given run, thereby permitting a direct comparison between the heat-transfer coefficient for the MACOR hemispheres to those for the quartz and Pyrex hemispheres. To account for small variations in the radii of the hemispheres, which were measured on an optical comparator at a magnification of 20, the results are compared in the form $C_h/(p_{t,2}/r_n)^{1/2}$, where the heat-transfer coefficient $C_h = q_{t,2}/(T_{t,2} - T_s)$. Four runs were made in the Mach 10 Tunnel covering the range of Reynolds number (reservoir pressure) for this facility, with the last run being a repeat of the first; two runs were made in the CF_4 Tunnel. Calibrations performed before and after the test series revealed the resistance of four of the five gages remained constant to within 1% and the other to within 3%. The temperature coefficient of resistance increased 0.9-1.4% for all gages during the test series. This relatively good gage stability is attributed to improved annealing techniques, as compared to Ref. 1, and illustrates the low level of solid contaminants in the flow of these tunnels for these tests.

The primary reason for testing such small hemispheres was to allow several hemispheres to be tested simultaneously without tunnel blockage. Another reason was to obtain heating rates and surface temperatures indicative of the maximum values expected in these facilities. For $t \leq 1.4$ s, where $t = 0$ is defined as the moment the thin-film gages experience an increase in their output during their movement into the flow, surface temperatures up to 570 K were experienced. The maximum correction to the heat-transfer rate required to account for the variation of substrate thermal properties with temperature was 16, 33, and 59% for MACOR, quartz, and Pyrex, respectively. Even with these large corrections, C_h varied less than ±2.5% for the MACOR and quartz hemispheres and ±5% for the Pyrex hemisphere over the time interval $0.5 \leq t \leq 1.4$ s in the Mach 10 Tunnel. These relatively small variations in C_h lend credibility to the approximate method derived in Ref. 1 to account for the variation of β with temperature. Also, the time histories gave no hint that the hemispheres violated the assumption of a semi-infinite substrate.[1-3] The results presented herein correspond to $t = 0.6$ s.

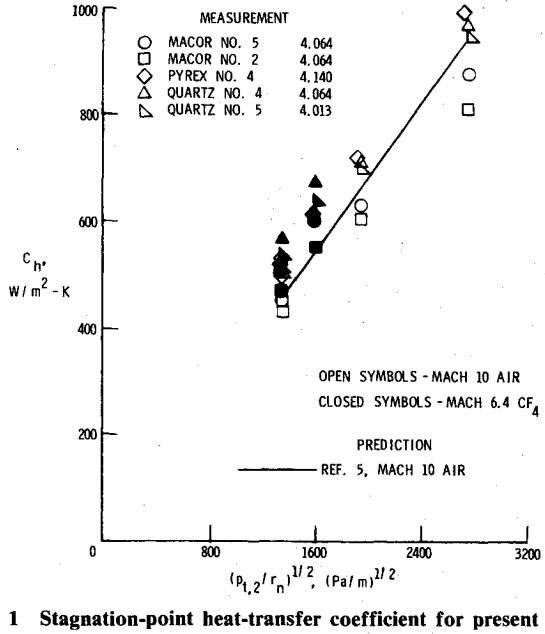

Fig. 1 Stagnation-point heat-transfer coefficient for present hemispheres as a function of velocity gradient.

Results

The heat-transfer coefficient is plotted in Fig. 1 as a function of the velocity gradient term $(p_{t,2}/r_n)^{1/2}$. Viscous and possible vibrational relaxation effects within the shock layer of the hemispheres are assumed to be the same magnitude for each hemisphere for a given run. The average value of $C_h/(p_{t,2}/r_n)^{1/2}$ for the two quartz hemispheres ranged from 1.10 to 1.15 times the average for the two MACOR hemispheres for the six runs; the average of this ratio was 1.135 for these runs in both facilities and 1.125 for the ratio of Pyrex to MACOR. Because the thermal properties for quartz and Pyrex are believed to be accurately known, the present results demonstrate that values of $\dot{q}$ determined with the method of Ref. 1 for thin-film gages with MACOR substrates will be too small by approximately 13%. [Note that $\dot{q} \propto \beta_s$, where the thermal product for the substrate $\beta_s = (\rho_s c_s k_s)^{1/2}$.] Based on these findings, the following simple expression is recommended to determine $\beta_{s,0}$ for a MACOR substrate at ambient or prerun conditions ($\beta_{s,0}$ in W-s$^{1/2}$/m^2-K)

$$\beta_{s,0} = 1816.6 + 0.6303 T_0 \quad 294 \leq T_0 \leq 312 \text{ K} \tag{1}$$

where the variation in β with temperature is accounted for using the expression

$$\dot{q}_{\beta_{s(T)}}(t) = \dot{q}_{\beta_{s,0}}(t)\,[1 + 6.38 \times 10^{-4} \Delta T_s(t)] \quad T_s \leq 450 \text{ K} \tag{2}$$

The value of $\beta_{s,0}$ for MACOR presented in Ref. 1 was obtained from information supplied by the manufacturer of MACOR, from the results of a study using the comparative method, and from a study using a step-input heat-rate method. (See Appendix A of Ref. 1). These sources, which agreed reasonably well with one another, were selected over experimental results furnished by Wittliff.[9] The present study, using yet another method to determine the value of $\beta_{s,0}$ for MACOR, shows the error of the selection made in Ref. 1 since $\beta_{s,0}$ from Eq. (1) is within 1% of the value determined in Ref. 9. The confidence level in Eq. (1) is further enhanced by the re-

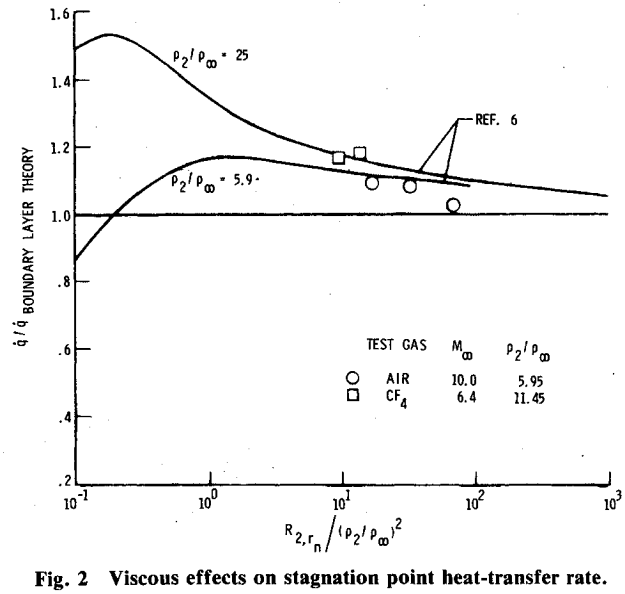

Fig. 2 Viscous effects on stagnation point heat-transfer rate.

cent study of Ref. 3, the results of which are also within 1% of Eq. (1). Thus, Eqs. (1) and (2) are expected to provide an accurate determination of $\dot{q}$ from thin-film gages on MACOR substrates, which, in turn, allows detailed heating distributions to be measured accurately on complex models in conventional hypersonic wind tunnels that are not possible with transient calorimeter techniques, as demonstrated in Ref. 3.

Because of the small size of the hemispheres, corresponding to relatively low values of Reynolds number based on nose radius, the present results also provide information on viscous effects on stagnation-point heating. As the Reynolds number is reduced, classical boundary-layer theories (see, for example, Ref. 5), initially underestimate heating as viscous effects become significant, then progressively overestimate heating as slip effects become significant. This trend is well documented in the literature and is illustrated by the curves in Fig. 2 which were taken from Ref. 6. Each of the five hemispheres revealed an effect of Reynolds number on stagnation-point heating in the Mach 10 Tunnel, with $C_h/(p_{t,2}/r_n)^{1/2}$ increasing about 8% as R_{∞,r_n} decreased from 32.5 to 7.9×10^3. Viscous effects were also evident in the comparison of measured heating for the quartz hemispheres to that predicted by the theory of Fay-Riddell.[5] This comparison is shown in Fig. 2 where the ratio of measured-to-predicted stagnation-point heating is plotted as a function of the post-shock Reynolds number and the normal shock density ratio. Now, since the thin-film element covers the stagnation region within 10 deg of the stagnation point, the measured heating rate will be lower than the stagnation-point value by 1-2%. Possible vibrational nonequilibrium effects may also tend to lower the heating. Nevertheless, viscous effects are observed in Fig. 2 to cause the measured heating to exceed classical boundary-layer prediction by up to 10% for the present Mach 10 flow conditions in air. Measured heating rates in Mach 10 air also exceeded values predicted with a code[7] that solves the Navier-Stokes equations but by no more than 5% (experimental uncertainty). Measured heating rates in Mach 6.4 CF_4 presented in Fig. 2 are nondimensionalized by values predicted using a boundary-layer code and the thermodynamic properties for CF_4 given in Ref. 8. These CF_4 results are of particular interest since they simulate the increase in shock strength that occurs for a blunt body during reentry due to dissociation within the shock layer. The experimental results of Fig. 2 show the influence of viscous effects on heating increases substantially with increasing shock strength for the present range of Reynolds number, in agreement with the predictions of Ref. 6.

References

[1]Miller, C. G., "Comparison of Thin-Film Resistance Heat-Transfer Gages with Thin-Skin Transient Calorimeter Gages in Conventional Hypersonic Wind Tunnels," NASA TM 83197, Dec. 1981.

[2]Schultz, D. L. and Jones, T. V., "Heat-Transfer Measurements in Short-Duration Hypersonic Facilities," AGARD-AG-165, Feb. 1973.

[3]Wannenwetsch, G. D., Ticatch, L. A., Kidd, C. T., and Arterbury, R. L., "Results of Wind Tunnel Tests Utilizing the Thin-Film Technique to Measure Wing Leading-Edge Heating Rates," AEDC-TR-83-50, May 1984.

[4]Miller, C. G., "Measured Pressure Distributions, Aerodynamic Coefficients, and Shock Shapes on Blunt Bodies at Incidence in Hypersonic Air and CF_4," NASA TM 84489, Sept. 1982.

[5]Fay, J. A. and Riddell, F. R., "Theory of Stagnation Point Heat Transfer in Dissociated Air," *Journal of Aeronautical Sciences*, Vol. 25, Feb. 1958, pp. 73-85, 121.

[6]Gilbert, L. M. and Goldberg, L., "A Reynolds Number Scaling Theory for Hypersonic Ablation," AIAA Paper 67-155, Jan. 1967.

[7]Gnoffo, P. A., "A Vectorized, Finite-Volume, Adaptive Grid Algorithm Applied to Planetary Entry Problems," AIAA Paper 82-1018, June 1982.

[8]Sutton, K., "Relations for the Thermodynamic and Transport Properties in the Testing Environment of the Langley Hypersonic CF_4 Tunnel," NASA TM 83220, Oct. 1981.

[9]Wittliff, C. E., private communication, Calspan Advanced Technology Center, Buffalo, N.Y.

An Adaptive Finite Element Technique for Plate Structures

M. E. Botkin*
General Motors Research Laboratories
Warren, Michigan

Introduction

THERE have been several papers written on the subject of adaptive mesh generation;[1-3] however, few have emphasized the complete model building process.[4] The emphasis in Refs. 1-3 tends to be the determination of the solution quantity used as a refinement criterion, but such systems do not automatically obtain an initial mesh or carry out the refinement process. The process described by Shephard[4] addresses the abovementioned features, but relies heavily on interactive graphics to tailor the refined mesh. It was desired to develop a technique that could be used with shape optimization,[5] as well as to have an efficient modeling technique that relieves the analyst of much of the work of finite element modeling. For this reason, three major features were required: 1) mesh refinement based upon an initial solution, 2) efficient modeling of the initial mesh, and 3) "blackbox" operation.

Structural components subject to bending deformations are of particular interest to the automotive industry. None of the authors of mesh refinement papers have treated bending problems, probably due to the undesirable characteristics of bending-type finite elements. An example with bending has been included in this Note.

Mesh Refinement

The mesh refinement process is based upon the variation in strain energy density (SED) as a measure of the error in an element. In order to show this, consider the relationship[4] expressing the error in a solution quantity in an element in terms of the variation in that quantity

$$|V-V_I|_e \le C_j h_e^k |D^k V|_e \tag{1}$$

where V is some exact solution quantity (stress or SED), V_I the computed value, C_j a proportionality factor, h_e the element size, and D^k a differential operator of order k (the order of the element). For constant-strain elements ($k=1$), the error is proportional to the element size times the first variation in the solution quantity. The following empirical relationship has been proposed in Ref. 4 for determining a level of SED variation above which the elements will be subdivided:

$$CV=\overline{\Delta E}+\beta(\Delta E_{\max}-\overline{\Delta E}) \tag{2}$$

in which CV is the SED difference cutoff value, $\overline{\Delta E}$ the average SED variation for all elements, $\Delta E_{\max}$ the maximum SED variation in any element, and β a parameter to be selected based upon the problem but generally lying between 0 and ½.

Obviously, the accuracy due to any refinement is unknown in advance. Although numerous papers have been written on error estimates of total strain energy (many of which have been noted in Ref. 6), this work cannot be readily extended to stresses and displacements. For the case of shape optimization, it is desired to have a conservative estimate of the converged finite element solution. This information may be obtained using a linear extrapolation technique, such as graphically represented by Fig. 1. This is a typical relationship

Received Oct. 6, 1983; revision received June 21, 1984.

*Staff Research Engineer, Engineering Mechanics Department.